Ecological Modelling 455 (2021) 109619

Contents lists available at ScienceDirect

Ecological Modelling

journal homepage: www.elsevier.com/locate/ecolmodel

On the use of ABACUS high resolution glider observations for the assessment of phytoplankton ocean biomass from CMEMS model products

Giuseppe Aulicino [a,*], Cinzia Cesarano [b], Mohamed Zerrouki [c], Simon Ruiz [d], Giorgio Budillon [a], Yuri Cotroneo [a]

[a] Dipartimento di Scienze e Tecnologie, Università degli Studi di Napoli Parthenope, Napoli, Italy
[b] Dipartimento di Scienze della Vita e dell'Ambiente, Università Politecnica delle Marche, Ancona, Italy
[c] National School for Marine Sciences and Coastal Management, Algiers, Algeria
[d] Instituto Mediterráneo de Estudios Avanzados, IMEDEA (CSIC-UIB), Esporles, Spain

ARTICLE INFO

Keywords:
Glider high resolution measurements
Phytoplankton biomass monitoring
Chlorophyll-a concentration modelling
Western Mediterranean sea

ABSTRACT

Ocean biomass distribution has a growing importance in the world economy as a global strategic reserve, due to environmental and industrial applications and its variability related to climate change. Satellite imagery allows multi-resolution methodologies to obtain estimation, and hopefully classification, of biomass content over sea surface. This information is largely used in numerical simulations and nowadays represents an important contribute to future projections. Nevertheless, satellite, models and classical in situ monitoring resolution/accuracy sometimes cannot provide data at the finer spatial scales needed to describe the complex three-dimensional water column system. On the other hand, glider surveys allow scientists to collect observations of ocean phenomena at very high resolution along the water column, to assess numerical simulations reliability and, eventually, to assimilate these data into ocean models. In this study, we present a quantitative comparison between the glider observations collected in the Algerian Basin (Western Mediterranean Sea) during the ABACUS surveys from 2014 to 2018, and the daily outputs of two co-located CMEMS model products (i.e., GLB and IBI). The achieved results point out that model products are well correlated with glider potential temperature measurements but they still need improvements to provide a correct representation of the chlorophyll concentration variability in the study area. Generally, IBI daily simulations present higher linear correlation with concurrent glider in situ data than GLB ones. IBI products also reproduce better the pattern of the local maxima of chlorophyll concentration across the Algerian Basin. Nevertheless, they largely underestimate glider chlorophyll measurements and present significant differences that limit their capability to reproduce its upper ocean concentration that is needed for accomplishing advanced ecological studies.

1. Introduction

Natural capital refers to the stock of natural assets, including soil, air, water and all living things, generating a wide range of ecosystem 'goods and services' which enable humans to live, and produce value or benefits to people directly or indirectly (Barbier, 2019). These assets are currently under pressure all over the globe, resulting in changes in the function of several ecological systems and in the benefits derived by people (Leach et al., 2019). Ecosystem services are the direct and indirect contributions of ecosystems to human well-being, so that its valuation is now widely recognised as a useful, though sometimes neglected, tool for conservation and management in the terrestrial and marine environment (MERP 2019). Moreover, understanding marine environment functions and how we alter them is essential for preparation of the basic concepts for conservation and sustainable use of marine biodiversity.

In the last decades, contemporary threats to marine biodiversity due to increasing anthropogenic pressure (e.g., climate change, pollution and unsustainable fishing) are likely to cause unpredictable changes in the provision of marine ecosystem services. Marine ecosystems are amongst the most productive environments in the world and their stocks of natural capital offer a bundle of vital ecosystem services (MERP 2019). In particular, ocean biomass distribution has a growing importance in the world economy as a global strategic reserve. Understanding how the marine environment functions to maintain natural capital to provide goods and services, and how we may be altering it directly (e.g.,

* Corresponding author.

https://doi.org/10.1016/j.ecolmodel.2021.109619
Received 1 September 2020; Received in revised form 18 May 2021; Accepted 19 May 2021
Available online 3 June 2021

by over exploitation) or indirectly (e.g., through climate change) is essential for a sustainable long-term future for the marine environment and humans (Picone et al., 2017).

The alteration of algal community composition and distribution represents an important bio-indicator of several climate-driven effects on environmental forcing and marine ecosystem equilibrium (Sathyendranath et al., 2014). Chlorophyll-*a* (hereafter Chl-a) concentration measurements play a fundamental role in marine ecosystem research as excellent proxy for phytoplankton biomass and seawater trophic conditions (Sathyendranath et al., 2017). The information on Chl-a patterns at global and regional scales is usually pursued through several approaches, e.g., modelling studies, in situ measurements and satellite sensors (Sammartino et al., 2018).

Ocean models has brought to bear a vast range of skills and experience from empirical scientists to modellers to socio-economists with the aim of understanding how we can maximise the benefits we get form our seas through trade-offs between economic, ecological and cultural activities and services while maintaining clean, safe and healthy seas, and the living natural capital they contain (MERP 2019).

The ocean, however, is difficult to monitor, to study and to model, as it is characterized by multiple factors, including complex processes occurring on several spatial and temporal scales, impressive biodiversity and serious governance issues. To obtain a complete view of such processes and provide valuable input data to models, ocean scientists aim at collecting data over long time periods and at the higher temporal and spatial resolution feasible. Historically, these measurements were continually provided by fixed sensors (e.g., moorings) and ship oceanographic campaigns, obtaining measurements which are mostly one dimensional, i.e., at a single point along depth, or two dimensional through a cross section, i.e., data along depth on a ship track (Castagno et al., 2020). Furthermore, using classical methodologies for ocean dynamics monitoring and biomass inventory is usually time consuming and expensive, while results can be affected by synopticity and spatio-temporal scale issues. Additionally, progress in numerical modelling also demonstrated the importance of mesoscale and fine-scale processes in shaping the biochemical cycles and biodiversity distribution (Lévy et al., 2018). Since scale interactions are ubiquitous, it is then of crucial importance to gain insight simultaneously into the large-scale circulation, the mesoscale dynamics and the sub-mesoscale processes. Unfortunately, reaching this objective using conventional cruise strategies is not straightforward, leading to a lack of in situ observations of fine-scale processes. These difficulties increase due to the lack, in some cases, of available open-source data (Di Luccio et al., 2020).

Since 1970s, the availability of satellite imagery allowed the development of new methodologies to obtain a global estimation, and hopefully classification, of biomass content over sea surface (e.g., Strömberg et al., 2009; Groom et al., 2019), also in combination with traditional in situ measurements (e.g., Aulicino et al., 2016; Rivaro et al., 2017; Misic et al., 2017; Mangoni et al., 2017; Rivaro et al., 2019a, 2019b). Furthermore, 25 years of progress in radar altimetry improved our capability of monitoring and understanding ocean circulation at large and mesoscales, but for the fulfillment of stringent requirements of observing sea level rise and its acceleration (Abdalla et al., 2021; Buonocore et al., 2020).

Due to their synoptic view, satellite observations partly fill the gap between large- and fine-scale dynamics. For many years, surface temperature and ocean colour products have been effectively used providing a greatly increased coverage of the ocean at different spatio-temporal scales. Nowadays these products represent an important contribution to ocean studies and are profitably used for assimilation in numerical simulations (Payne et al., 2019). Nonetheless, their measurements give us information only about the near surface pattern and provide a 2D (latitudinal/longitudinal) view of the ocean without describing what happens in the water column.

Considering the light penetration depth in the seawater, for example, satellite Chl-a represents only one fifth of the total Chl-a content within the euphotic zone, ignoring the algal biomass variability at deeper layers (Morel and Berthon, 1989). Still, as for classical in situ measurements, satellite products are often limited in resolving the large spatial and temporal variability of ocean biomass distribution and dynamics (e.g., neglecting the small- or mesoscale) because of their intrinsic characteristics (e.g., revisiting time, swath width, pixel resolution). Thus, they are not able (alone) to provide the high resolution detail of the complex three-dimensional ocean structure that is needed by ocean modellers for an improved initialization (and/or validation) of their numerical simulations. Additionally, most of satellite data do not reach the adequate resolution and quality when approaching the coast.

To overcome this limitation, several works attempted to reconstruct the sub-surface Chl-a field (and/or the column-integrated primary production) from surface satellite observations through different approaches including statistical methods (e.g., Morel and Berthon, 1989; Buongiorno Nardelli et al. 2006; Buongiorno Nardelli et al., 2017), machine learning techniques (e.g., Gueye et al., 2014; (Sauzède et al., 2016)) and neural network methods (e.g., Scardi et al., 2001; Richardson et al., 2002; Sammartino et al., 2018; (Buongiorno Nardelli, 2020)). Although several factors affect the successful extrapolation of the vertical structure from its surface pattern, in temperate areas, as the Mediterranean Sea, the existence of a strong seasonality makes the Chl-a vertical structure rather predictable (Sammartino et al., 2018). On the other hand, these products are usually validated versus climatological information and infer a smoothed representation of the punctual 3D structure of the ocean that partially improve the very sparse water column in situ information. Moreover, predicted Chl-a spring bloom can be significantly modified by eddy-driven slumping of density gradient at basin scale (Mahadevan et al., 2012).

As a result, a better design of sampling strategies and an enhanced resolution of data both in space and time are of fundamental importance to capture the observed phenomena along ocean depth. Lagrangian instruments provided then additional information to complete the description of the ocean variability but faced new limitations. This is especially the case of the Algerian Basin (hereafter AB) where Argo floats residence times, for instance, are very short (Taillandier et al., 2020) owing to the large density gradients and the associated strong currents (Poulain et al., 2012; Bouzaiene et al., 2018).

Recently, the advent of autonomous underwater vehicles (hereafter AUV) has enabled a complementary data acquisition approach and a higher accuracy and sampling resolution for a given region of interest, such as the AB (Aulicino et al., 2018; Cotroneo et al., 2019). This could address the pressing need amongst ocean scientists and modellers to efficiently and effectively collect the high resolution data which are expected to improve our monitoring and estimating capability of the phytoplankton ocean biomass stocks. In fact, AUV observations can represent an unprecedented opportunity to investigate the very fine-scale ocean processes and provide modellers information useful to reduce the grid size below a few hundred meters and properly resolve the ocean dynamics (Garreau et al., 2020). This is particularly important in specific ocean areas, e.g., the Mediterranean Sea, which are known for being characterized by intense and contrasting dynamics. Previous studies, for instance, emphasized that very high resolution in situ data can be essential to identify the effects of frontal instabilities generating Chl-a filaments, or those of eddies acting both as biological barriers and drivers of plankton diversity (Cotroneo et al., 2016; Bosse et al., 2017; Ruiz et al., 2019; Sanchez-Roman et al., 2019; Garreau et al., 2020).

In this study, we i) present the high resolution glider ocean observations (potential temperature, salinity, Chl-a) collected in the AB (south-western Mediterranean Sea) between 2014 and 2018 during a series of dedicated glider surveys (Cotroneo et al., 2019), and ii) compare this information with co-located numerical simulations outputs provided by Copernicus Marine Environment Monitoring Service (CMEMS). The main goal is to evaluate the CMEMS daily products capability to give us reliable information about the Chl-a concentration of the water column in one of the most important areas of the

Mediterranean Sea (i.e., the AB), and strengthen the importance of glider high resolution data for improving our knowledge of the study area phytoplankton biomass and seawater trophic conditions.

The paper is structured as follows: study area, datasets and methodologies are described in Section 2; results are presented and discussed in Section 3; concluding remarks are summarized in Section 4.

2. Study area and datasets

2.1. The Algerian Basin

The Mediterranean Sea is a semi-enclosed evaporation basin, largely driven by the thermohaline circulation, which exhibits many processes of primary interest in the functioning of the global ocean (Robinson and Golnaraghi, 1994) and presents an high connection amongst its sub-basins (Celentano et al., 2020). It is a relatively restrained and accessible area, thus providing an excellent opportunity to investigate a large amount of geophysical and biochemical oceanic features (Barceló-Llull et al., 2020), from long term changes in water properties (Fusco et al., 2008; Krauzig et al., 2020) to the possible interaction between ocean properties and anthropogenic impact on the marine environment (i.e., marine litter dispersion, Zambianchi et al., 2017).

The AB is a wide and deep transit region of the south-western Mediterranean that occupies a large area between the Balearic Islands, the Algerian coast and the Sardinia Channel (Fig. 1). It is characterised by the presence and interaction of different water masses (e.g., fresh surface Atlantic Waters, more saline resident Mediterranean Waters, intermediate Levantine Intermediate Waters, Western Mediterranean Deep Waters), whose properties varies according to different stages of mixing, geographical position, and residence time (Millot et al., 1999). The general circulation of these water masses is strongly influenced by both an intense inflow/outflow regime and complex circulation patterns (Pascual et al., 2013; Aulicino et al., 2019), which act at different spatial and temporal scales, including basin-scale, sub-basin-scale, and mesoscale (Robinson and Golnaraghi, 1994; Vidal-Vijande et al., 2011), allowing multiple interactions and a high seasonal and interannual variability in the basin (Fusco et al., 2003).

Typically, Atlantic Waters entering from the Strait of Gibraltar flows eastward carried by the Algerian Current (AC). Due to complex hydrodynamic processes, AC becomes unstable along its path and generates several meanders that usually evolve into fresh-core mesoscale structures, i.e., eddies and filaments (Fig. 1). These structures propagate downstream and promote water mass mixing all over the AB (Ruiz et al., 2002; Taupier-Letage et al., 2003; Testor et al., 2005; Escudier et al., 2016; (Bosse et al., 2016); Pessini et al., 2018, 2020), impacting the distribution of physical properties, especially at surface and intermediate depths (Pascual et al., 2013).

This dynamic and very energetic activity has also marked repercussions on biogeochemical properties (Cossarini et al., 2012; Coppola et al., 2018) which modulates biological activity and ecosystems (Taupier-Letage, 1988; Taupier-Letage et al., 2003) through nutrient injection (removal) into (out of) the euphotic layer (Olita et al., 2011; Cotroneo et al., 2016). These processes contribute to algal blooms and primary production rates, also leading, locally and episodically, to unexpectedly high Chl-a or primary production values for the Mediterranean region (Robinson, 1983; Raimbault et al., 1993; Mahadevan et al., 2012).

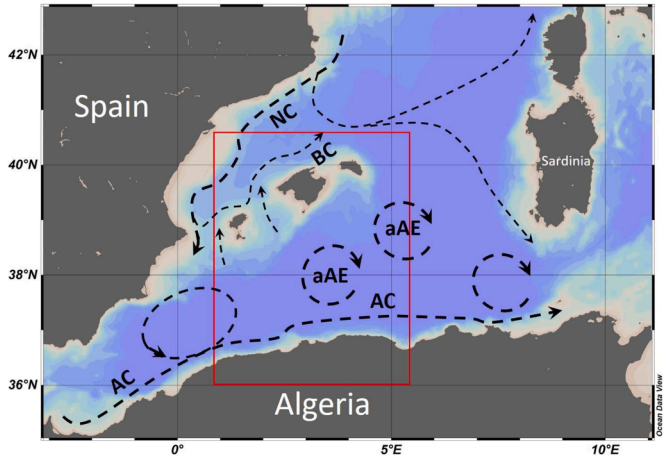

Fig. 1. Schematized representation of the surface circulation in the western Mediterranean Sea (adapted from Poulain et al., 2012 and Heslop et al., 2012). The red box identifies the sub-region in Fig. 2, i.e. the Algerian Basin sector south of the island of Mallorca. Northern Current (NC), Balearic Current (BC), Algerian Current (AC) and mean position of recurrent anticyclonic Algerian Eddies (aAE) are labelled.

2.2. ABACUS glider dataset

Gliders are AUVs able to provide high resolution physical and biochemical measurements along the water column, controlling their buoyancy to allow vertical motion (Webb et al., 2001).

Four deep SLOCUM G2 glider missions were carried out in the AB between 2014 and 2018 by Università degli Studi di Napoli Parthenope, in collaboration with Balearic Islands Coastal Observing and Forecasting System (SOCIB) and the Mediterranean Institute for Advanced Studies (IMEDEA CSIC-UIB).

A total of 14 glider deep transects were completed during the four ABACUS projects realizing a repeated monitoring line between the island of Mallorca and the Algerian coast (Fig. 2). Each mission had an average duration of about 40 days and was mainly carried out during fall (i.e., between September and December 2014–2018) or spring (in May-June 2018), as summarized in Table 1. All the glider surveys were conducted along neighbouring SARAL/AltiKa (ABACUS 1 to ABACUS 3) and Sentinel-3A (ABACUS 4) satellite groundtracks. The timing of the glider missions were also accurately planned to be almost simultaneous with the satellite passages in order to optimize the synopticity between in situ and remote sensed observations. Additionally, in 2014 and 2015, after the realization of the defined transects, the glider was deviated

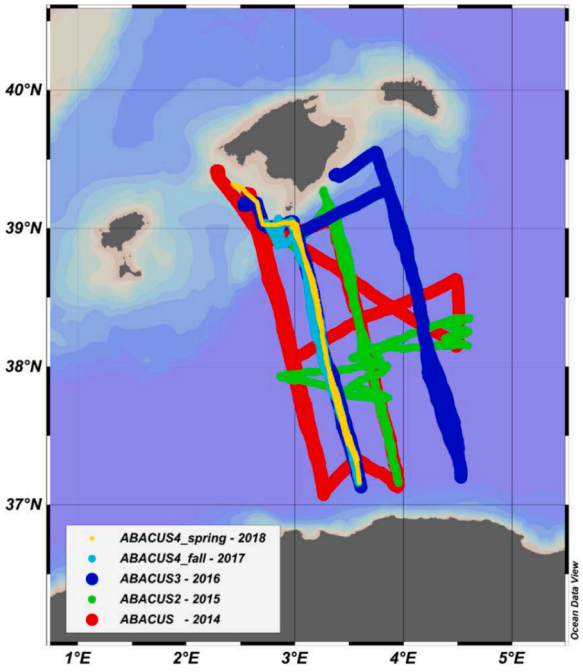

Fig. 2. Glider casts positions during the ABACUS missions at sea in autumn 2014 (red), 2015 (green), 2016 (blue), 2017 (cyan), and spring 2018 (yellow).

Table 1
ABACUS glider missions details: periods of activities at sea (from – to) and number of acquired water column casts.

Mission	From	To	Casts
ABACUS	15 Sep 2014	19 Dec 2014	420
ABACUS 2	19 Oct 2015	11 Dec 2015	1100
ABACUS 3	5 Nov 2016	23 Dec 2016	794
ABACUS 4	16 Nov 2017	11 Dec 2017	505
ABACUS 4 spring	15 May 2018	7 Jun 2018	497

from the monitoring line to sample specific mesoscale structures identified through near real time satellite altimetry and sea surface temperature maps.

During data collection, gliders dived with an angle of 26° with the sea surface, following a typical saw-toothed navigation pathway to a maximum depth of 975 m, at an average vertical speed of 0.18 ± 0.02 m/s with a resulting net horizontal velocity of about 0.36 m/s. All the glider platforms used during the ABACUS surveys were equipped with the same instrumentation, i.e., a glider-customized CTD by Seabird measuring temperature, conductivity/salinity and pressure/depth; a two-channel combo fluorometer sensor by WetLabs (for Chl-a concentration and turbidity measurement); and an oxygen optode by AADI to measure absolute oxygen concentration and saturation.

In general, temperature, salinity and oxygen data were sampled to full diving depth (0–975 m depth), while the acquisition of the other optical parameters ceased at 300 m depth. Taking progressively advantage of the lesson learned, the glider was programmed to reach the surface at different rates and spatial resolution during the different ABACUS missions; this resulted in a variable resolution of sampling, especially in the very surface layer (0–20 m depth), which ranges between 2 and 8 km. However, physical parameters were generally sampled at 1/2 Hz on both descending and ascending phase, resulting in a vertical resolution of 0.4 m along the water column; oxygen information was acquired at 1/4 Hz (vertical resolution of 0.8 m); turbidity and Chl-a were sampled at 1/8 Hz down to 150 m depth and at 1/16 Hz from that level down to 300 m depth (i.e., with a vertical resolution of 1.6 and 3.2 m respectively).

Details and motivations of data acquisition strategy during the different surveys, as well as quality control procedures and glider technical information (e.g., setting, maintenance, calibration, permission operations), are fully described in Cotroneo et al. (2019) and references therein. A deep quality control was applied to glider data in order to exclude any issue in the observations and support the complete reliability of the in situ dataset. In particular, a double check was carried out in order to verify that the thermal leg correction (Garau et al., 2011) was correctly applied to glider salinity measurements. The final glider dataset is available through an unrestricted repository at https://doi.org/10.25704/b200–3vf5 (Budillon et al., 2018). Please notice that the analysis of oxygen data provided in the repository is not included in the present study which focus on Chl-a concentration as one of the main marine ecological parameters for assessing phytoplankton biomass and trophic conditions.

Comparing gridded forecasts with observations at point locations needs the use of super-observations (upscaled observations). There are several methods available to upscale observations, from simple averages, distance weighted-averages, error (observational and representativity) weighted methods (e.g. Daley, 1991), to multi-variate statistical methods (e.g., Pardo-Iguzquiza, 1998). In this study, hydrographic and Chl-a profiles from gliders have been sorted, depending on their matching date and location with the model gridded outputs described in Section 2.3, then, the selected profiles have been averaged to one mean profile per day, which is used for co-location with model values. Potential temperature values have been computed through the algorithm coded in the Ocean Data View (ODV) software.

2.3. CMEMS data

Data collected during glider field activities were compared with co-located products provided by two CMEMS models which include daily Chl-a concentration information, i.e., the Global Reanalysis (hereafter GLB) and the Iberian Biscay Ireland Regional Seas Ocean Reanalysis (IBI). In particular, the analysed products include the GLOBAL_REANALYSIS_BIO_001_029 and the IBI_REANALYSIS_BIO_005_003 for Chl-a information, and the GLOBAL_REANALYSIS_PHY_001_030 and the IBI_MULTIYEAR_PHY_005_002 for physical parameters (i.e., physical temperature, salinity and derived variables), as summarized in Table 2. The GLB biogeochemical hindcast for global ocean is produced at Mercator-Ocean (Toulouse, France) using PISCES biogeochemical model (Aumont et al., 2015) available on the NEMO modelling platform. It provides 3D biogeochemical fields for the time period 1993–2019 at 1/4° and on 75 vertical levels with a resolution of 1 m near the surface and 200 m in the deep ocean. The model is forced offline by daily 3D fields from the ocean dynamical simulation FREEGLORYS2V4 produced at Mercator-Ocean and ERA-Interim atmosphere parameters produced at ECMWF at a daily frequency. There is no data assimilation, neither physical data nor biogeochemical data (Perruche et al., 2019). The available outputs include daily and monthly 3D mean fields interpolated on a standard regular grid in NetCDF format. On the global ocean, an RMS difference of 0.371 μg/l at sea surface has been estimated for the modelled chlorophyll in comparison with daily satellite observations (Perruche et al., 2019). From this dataset we extracted Chl-a concentration daily values in coincidence with all the ABACUS glider transects between Mallorca and the AC.

As for GLB daily physical products, the CMEMS global ocean eddy-resolving 1/12° horizontal resolution (approximatively 8 km) 50 vertical standard levels reanalysis is based on the NEMO platform driven at surface by ECMWF ERA5 reanalyses. Observations are assimilated by means of a reduced-order Kalman filter, i.e., along track Sea Level Anomaly altimetry data, satellite Sea Surface Temperature, and in situ temperature and salinity vertical profiles. A 3D-VAR scheme provides a correction for the slowly-evolving large-scale biases in temperature and salinity (Fernandez and Lellouche, 2018). From this dataset we extracted potential temperature and salinity daily values co-located with glider profiles.

The IBI model provides a 3D high resolution biogeochemical multi-year product starting on January 1992 using an application of the PISCES biogeochemical model that is run simultaneously with the ocean physical IBI reanalysis. IBI daily and monthly mean products are provided at 1/12° horizontal resolution on 50 vertical levels. The biogeochemical model is initialized with a monthly climatology (using years 2010 to 2015) build from the Global Ocean Analysis Product (GLOBAL_ANALYSIS_FORECAST_BIO_001_028) at 1/4° horizontal resolution for the same starting month (Baladrón et al., 2020). From this dataset we extracted daily Chl-a concentration values for the time intervals of ABACUS gliders operations along the Mallorca-AC transects.

As for IBI daily physical products, the numerical core is based on the NEMO v3.6 ocean general circulation model run at 1/12° horizontal resolution in which altimeter data, in situ temperature and salinity vertical profiles and satellite sea surface temperature are assimilated (Baladrón et al., 2020).

From these datasets we extracted chlorophyll, and potential temperature and salinity, daily values co-located with glider profiles, respectively.

All the data have been accessed from http://marine.copernicus.eu on January 2021.

3. Results and discussion

The description of the water masses and their characteristics using the ABACUS underwater glider observations has been already given in previous studies (e.g., Aulicino et al., 2018; Cotroneo et al., 2019).

Table 2
CMEMS products included in this study.

Product	Spatial resolution	Vertical levels	Temporal resolution	Data assimilation
GLOBAL_REANALYSIS_BIO_001_029	1/4°	75	Daily	NO
IBI_REANALYSIS_BIO_005_003	1/12°	50	Daily	NO
GLOBAL_REANALYSIS_PHY_001_030	1/12°	50	Daily	YES
IBI_MULTIYEAR_PHY_005_002	1/12°	50	Daily	YES

Several authors also discussed the advantages of using glider data for identifying and monitoring mesoscale structures and evaluate their effects on the mixed-layer depth (hereafter MLD) and biochemistry (e.g., Niewiadomska et al., 2008; Ruiz et al., 2009; Olita et al., 2014; Cotroneo et al., 2016).

In this work, the high resolution in situ glider observations acquired during the ABACUS surveys realized in the AB during the 2014–2018 period have been analysed and compared to concurrent numerical simulations with a specific focus on Chl-a concentration measurements and estimates. The final goal is to understand to which extent we can obtain a reliable daily estimation of ocean phytoplankton biomass in the study area through the use of CMEMS models Chl-a outputs.

In fact, while gliders provide synoptic observations and help monitoring only the ocean area along their tracks, numerical simulations can complete this information over wide areas, especially when in situ monitoring systems are not available. Nevertheless, they need a proper validation in order to understand the error we commit when using the model products in place of in situ measurements.

3.1. Statistical analyses

Comparing ocean datasets obtained by different sources and methodologies (e.g., classical research vessel activities, AUV, remote sensing, numerical simulations) always requires an accurate statistical analysis. Here we compare datasets (i.e., CMEMS model outputs and ABACUS glider in situ observations) that differ in terms of methodological approach, spatial and temporal resolution, synopticity, and that usually are not compared as default. Thus, statistical information is needed to provide a quantitative analysis of the differences between these products.

Firstly, each glider profile collected from 2014 to 2018 has been compared to the co-located GLB and IBI ones, considering a subset of the available super-observed data from surface to 110 m depth, i.e., the maximum depth at which Chl-a data presented an interesting variability (see Figure 8d in Cotroneo et al., 2019). Statistics for the enquired parameters (i.e., potential temperature, salinity and Chl-a concentration) have been computed for both the full available dataset (Table 3) and the single glider surveys (Table 4).

The main results listed in Table 3 are also summarized in the Taylor diagrams shown in Fig. 3 which facilitate the comparative assessment of GLB (red dots) and IBI (blue dots) CMEMS models. These diagrams help to quantify the degree of correspondence between the modelled and the observed information in terms of three statistic descriptors, i.e., the Pearson correlation coefficient (R), the root-mean-square error (RMSE) and the standard deviation (SD).

Fig. 3 points out that the potential temperatures provided by both GLB and IBI products present an excellent linear correlation with glider in situ measurements ($R = 0.96$). Lower but acceptable statistics ($R \geq 0.66$) characterize the performances of both models in representing the upper ocean salinity. Conversely, GLB and IBI products present very different statistics when analysing Chl-a concentrations. The correlation results show that GLB values are completely unable to reproduce the co-located glider in situ observations ($R = 0.05$) while IBI ones agree in part with glider measurements ($R = 0.55$). This large discrepancy in models performance may be mainly ascribed to the different spatial resolution of the GLB (1/4°) and IBI (1/12°) Chl-a products, which is a significant

Table 3
Full dataset (2014–2018) statistics of the comparison between CMEMS GLB and IBI potential temperature (PT), salinity (S) and chlorophyll concentration (Chl-a) products, and the co-located ABACUS glider measurements. The number of compared points, the Pearson linear correlation coefficients (R), the root-mean-square errors (RMSE), the variance and mean values are listed.

	GLB			IBI		
	Chl-a	S	PT	Chl-a	S	PT
Number of points	8,770	20,183	20,183	16,688	16,688	16,688
Correlation coeff (R)	0.05	0.66	0.96	0.55	0.67	0.96
RMSE	0.27	0.29	0.80	0.22	0.34	0.92
Variance	0.05	0.10	8.34	0.07	0.11	10.17
Glider mean value	0.28	37.47	18.54	0.28	37.47	18.58
Model mean value	0.13	37.36	18.61	0.20	37.28	18.28

Table 4
Statistics of the comparison between CMEMS GLB and IBI potential temperature (PT), salinity (S) and chlorophyll concentration (Chl-a) products, and the co-located glider measurements collected during the 2014–2018 ABACUS campaigns. Parameters as in Table 3.

	GLB			IBI		
Sep - Oct 2014	**Chl-a**	**S**	**PT**	**Chl-a**	**S**	**PT**
Number of points	1,452	2,998	2,998	3,220	3,220	3,220
Correlation coeff (R)	−0.03	0.87	0.98	0.63	0.79	0.99
RMSE	0.31	0.20	0.94	0.26	0.26	0.70
Variance	0.07	0.13	20.55	0.11	0.14	20.86
Glider mean value	0.21	37.44	20.48	0.22	37.45	20.36
Model mean value	0.13	37.36	20.36	0.18	37.44	20.27
Nov - Dec 2014	**Chl-a**	**S**	**PT**	**Chl-a**	**S**	**PT**
Number of points	1,268	2,833	2,833	3,055	3,055	3,055
Correlation coeff (R)	−0.47	0.82	0.93	0.60	0.83	0.97
RMSE	0.30	0.20	0.63	0.16	0.24	0.47
Variance	0.04	0.12	3.02	0.04	0.13	3.10
Glider mean value	0.30	37.50	17.17	0.32	37.50	17.16
Model mean value	0.12	37.52	17.08	0.29	37.42	17.11
Oct - Dec 2015	**Chl-a**	**S**	**PT**	**Chl-a**	**S**	**PT**
Number of points	2,207	5,921	5,921	3,784	3,784	3,784
Correlation coeff (R)	−0.04	0.59	0.95	0.62	0.60	0.88
RMSE	0.30	0.43	0.85	0.24	0.52	1.55
Variance	0.05	0.09	7.01	0.07	0.10	7.54
Glider mean value	0.30	37.43	18.91	0.31	37.43	19.09
Model mean value	0.13	37.16	18.95	0.20	37.04	18.30
Nov - Dec 2016	**Chl-a**	**S**	**PT**	**Chl-a**	**S**	**PT**
Number of points	1,694	2,756	2,756	2,836	2,836	2,836
Correlation coeff (R)	−0.09	0.76	0.95	0.30	0.69	0.95
RMSE	0.20	0.24	0.71	0.20	0.24	0.71
Variance	0.02	0.06	4.96	0.02	0.07	4.84
Glider mean value	0.29	37.31	18.71	0.30	37.31	18.81
Model mean value	0.14	37.32	19.16	37.17	0.16	18.64
Nov - Dec 2017	**Chl-a**	**S**	**PT**	**Chl-a**	**S**	**PT**
Number of points	1,011	2,861	2,861	1,761	1,761	1,761
Correlation coeff (R)	0.22	0.07	0.82	0.24	0.31	0.91
RMSE	0.20	0.26	0.91	0.16	0.33	0.81
Variance	0.01	0.03	1.97	0.01	0.03	2.55
Glider mean value	0.28	37.53	18.50	0.26	37.50	18.92
Model mean value	0.12	37.54	18.77	0.21	37.42	18.25
May - Jun 2018	**Chl-a**	**S**	**PT**	**Chl-a**	**S**	**PT**
Number of points	1,160	2,818	2,818	2,035	2,035	2,035
Correlation coeff (R)	0.62	0.83	0.98	0.60	0.73	0.97
RMSE	0.22	0.23	0.39	0.21	0.23	0.36
Variance	0.07	0.12	4.20	0.06	0.10	3.06
Glider mean value	0.26	37.61	16.86	0.24	37.50	16.66
Model mean value	0.18	37.49	16.91	0.19	37.47	16.78

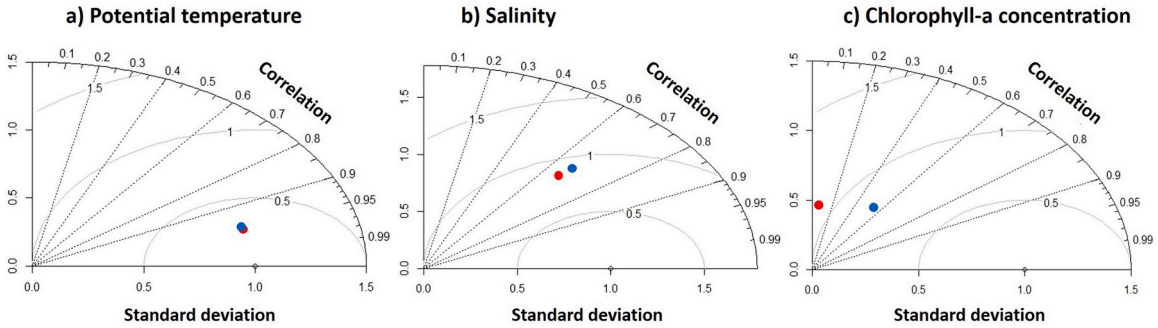

Fig. 3. Taylor diagrams present the comparative assessment of GLB (red dots) and IBI (blue dots) CMEMS models to ABACUS glider in situ measurements for a) potential temperature, b) salinity and c) chlorophyll concentration.

factor when comparing their outputs to glider data characterized by a variable but finer spatial resolution (i.e., between 2.8 and 8.4 km. See details in Cotroneo et al., 2019). Furthermore, even though both models underestimate Chl-a in situ observations, Table 3 points out that IBI usually provides better simulations also in terms of magnitude of Chl-a concentration.

Statistical analyses have been also realized for each single glider survey, in order to understand if particular in situ ocean conditions encountered during one of the missions at sea could have affected the overall statistical results. Results are summarized in Table 4.

As expected, also in this case the potential temperatures provided by both CMEMS models present a high correlation with glider data, the R values ranging between 0.82 (Nov - Dec 2017) and 0.98 (Sep - Oct 2014) and between 0.88 (Oct - Dec 2015) and 0.99 (Sep - Oct 2014), for GLB and IBI respectively.

This excellent agreement is not found in salinity as well. The linear correlation between GLB salinities and glider co-located observations is more variable, ranging between 0.59 and 0.87. Just as for potential temperature, the highest/lowest results are obtained for Oct - Dec 2015 and Sep - Oct 2014 surveys, respectively. A similar behaviour is found for IBI salinities, with R values ranging between 0.69 (Oct - Dec 2015) and 0.83 (Nov - Dec 2014). A special attention deserves the ABACUS 4 fall survey (Nov - Dec 2017). In fact, even though the potential temperatures match well, during this glider cruise we found no correlation with GLB salinities ($R = 0.07$) and a very low one with IBI ones ($R = 0.31$). These discrepancies are also evident in latitudinal sections of AB salinity between 0 and 110 m depth provided by the three datasets along the glider track. In particular, the analysis of the southward transect (16 - 27 November 2017, see Figure S4 in supplementary material) shows that GLB products do not reproduce correctly neither the spatial pattern nor the magnitude of in situ salinities observed by glider. On the other hand, although the IBI salinity pattern generally agrees with glider observations, the comparison of the latitudinal sections show that the model overestimates the intrusion of fresher surface water masses at the edges of the glider transect. This is particularly evident on the southern border where AC variability plays a critical role.

Considering the deep quality control dedicated to glider observations and thermal leg correction, we assume that this difference in correlation between potential temperature and salinity may be also ascribed to the higher degree of complexity in salinity model calculation due to the higher number of factors involved in the simulation (e.g., rivers, rainfall).

As for Chl-a concentration, single survey statistics confirm that GLB values are not correlated with the co-located glider observations, as shown by R values which range between −0.47 and 0.22, except than during the May 2018 mission at sea ($R = 0.62$). During this survey the thermocline was still deep and a weak stratification characterized the upper ocean, as confirmed by the lower values of the derivative of the potential density anomaly observed by the glider (see supplementary material). It is reasonable to speculate that the model represents the homogeneous water column better than in the other case studies, and thus provides a better estimation of the Chl-a pattern. It is also interesting to remark that the 2018 campaign is the only one carried out during spring time instead of fall period. Unfortunately, the available glider dataset does not allow further conclusions about. Additional in situ observations are necessary to provide more insights about seasonal dependency of models performance.

Conversely, IBI simulations agree better than GLB with in situ data for most of the glider surveys ($R \approx 0.6$). This is confirmed by the comparison of the upper ocean Chl-a latitudinal variability along the glider transects (see Section 3.2). Nonetheless, very low correlation coefficients are retrieved for Nov-Dec 2016 ($R = 0.30$) and Nov-Dec 2017 ($R = 0.24$) campaigns, even if the Chl-a simulations present reasonable mean and RMSE values.

All these findings suggested us to pay more attention to Chl-a concentration variability along the water column. Thus, additional statistical analyses at selected depths, between 1.5 m and 108 m, have been carried out for each available glider mission at sea. The achieved results are summarized in Figs. 4 and 5.

Generally, GLB and IBI potential temperature and salinity products have similar performances when compared to ABACUS glider measurements, with IBI simulations that report higher correlations with in situ data from 60 m to 110 m depth (Fig. 4). Conversely, Chl-a simulations present very different results for the two models, especially at shallower depths.

As for potential temperature, GLB and IBI model outputs have both an excellent correlation with glider measurements in the first meters of the water column (from surface to 30 m). As we move to deeper levels, GLB temperature correlation slowly decreases to $R = 0.62$ at 108 m depth, while IBI get worse between 40 m and 60 m depth and then improves again to reach $R = 0.89$ at the end of the analysed profile.

An opposite behaviour characterizes the salinity products, with lower performance at surface layer (e.g., $R = 0.45$ at surface) than at deeper levels (e.g., $R = 0.7$ at 54 m). In particular, IBI products show a constant increasing correlation with the highest values computed at 108 m ($R = 0.74$), while GLB correspondence with glider salinities decreases again from 60 m to 108 m.

Chl-a simulations present very different results for the two models, especially at shallower depths. Fig. 4 demonstrates that Chl-a variability along the water column is largely under-represented by CMEMS models daily products, and that only IBI outputs are able to reconstruct part of the glider observations, i.e. in the very surface layers ($R \approx 0.6$ in the upper 20 m).

However, for both models there are large changes in the correlation of the analysed parameters between 31 m and 61 m. Our hypothesis is that this may be associated to the correct simulation of the MLD that may have important repercussions on the modelling of the Chl-a distribution. The base of the mixed layer is characterized by rapid variation of the physical parameters and correspond to the depth at which the maximum of Chl-a is usually observed. Thus, we argue that both models

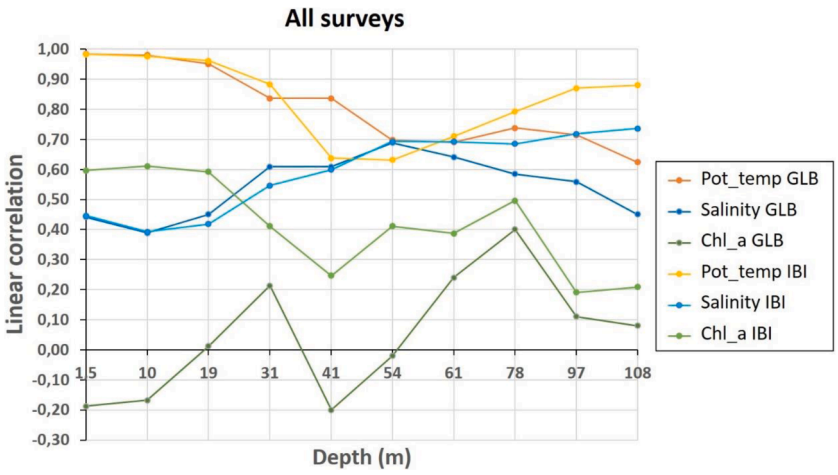

Fig. 4. Comparative assessment of GLB and IBI potential temperature, salinity and chlorophyll concentration products to co-located glider in situ measurements at selected depths. Linear correlation values refer to the entire dataset collected during the 2014–2018 ABACUS surveys.

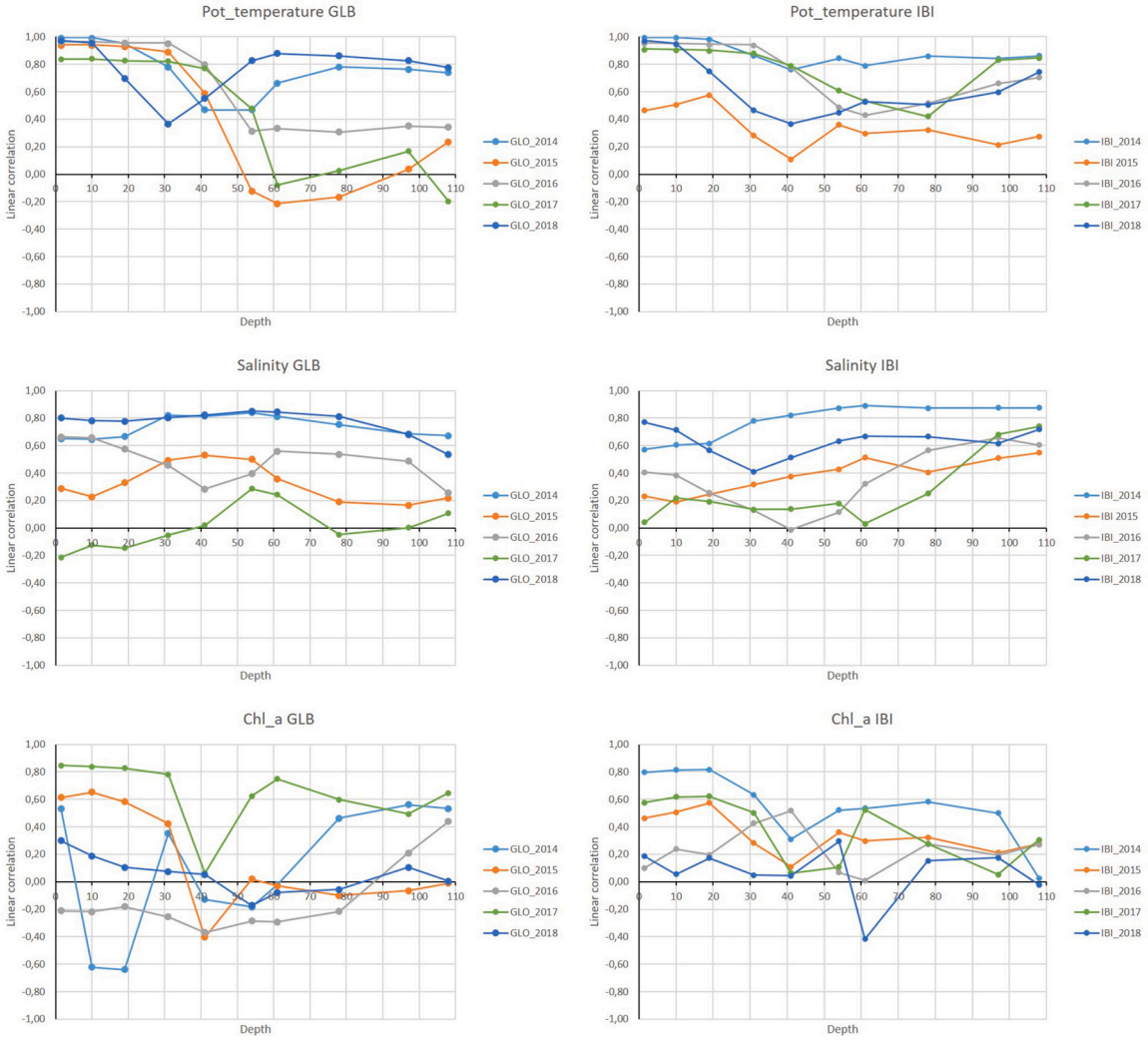

Fig. 5. Comparative assessment of GLB (left) and IBI (right) model potential temperature (top), salinity (middle) and chlorophyll concentration (bottom) products to co-located glider in situ measurements at selected depths for each year of the ABACUS series glider activities.

present some inconsistencies (more significant for GLB products) in the MLD positioning along the water column, mainly due to an inaccurate simulation of the potential temperature and salinity patterns, which imply consequent difficulties in representing the correct pattern and magnitude of Chl-a concentration. This hypothesis is also supported by the statistical results of the comparison carried out at selected depths

separately for each ABACUS survey (Fig. 5). As for potential temperature, it is difficult to assess that one model always performs better than the other. Generally, IBI products show a more regular correlation with in situ data and give better scores than GLB ones, but this is not true along the entire water column. At shallower depths (0 – 30 m), for example, GLB seems to reproduce the observed physical variability better than IBI during several surveys (e.g., ABACUS 2015). This information is also supported by latitudinal sections provided in the supplementary material. On the other end, GLB performance is often characterized by significant decrease in linear correlation with in situ measurements at depths deeper than 40 m. We argue that this behaviour strongly depends on the presence of specific ocean features, i.e., local phenomena at spatial scales which are not resolved by GLB model. The decrease of correlation with glider data in correspondence of the MLD, is generally noticeable for both models in Fig. 5. This means that, even though a general agreement is found, the potential temperature of the AB observed during the glider surveys is adequately represented by CMEMS daily models only in the very surface meters and in the deep layers, with important consequences on the simulations of the primary production descriptors, and of other properties associated to strong subsurface gradients, as discussed below.

Despite the encouraging results obtained through the overall statistical analyses, salinity simulations agree well only with a subset of the available in situ measurements (i.e., those collected during 2014 and 2018 surveys). Just as for temperature, GLB simulations give better results at shallower depths, IBI between 90 m and 110 m. The effect of MLD is still appreciable, even if its impact on the computed linear correlations is less evident than in potential temperature data.

As for primary production, unfortunately both IBI and GLB have serious issues in representing Chl-a daily variability measured by ABACUS gliders. IBI surface Chl-a concentrations seem better correlated with in situ observations in the upper layers (0–30 m) than in the rest of the water column. GLB products present less regular agreement and lower R-values. As discussed above, both models show an abrupt decrease of correlation with in situ data at about 30 m to 60 m, i.e., in correspondence of the expected MLD position. This decrease is clearly recognizable during all the glider surveys. Presumably, a different simulation of the MLD causes a shift in the location of the Chl-a maximum depth along the water column between models and in situ observations, and the consequent discrepancy in terms of measured/modelled concentrations. An indication of the location of the GLB and IBI modelled MLD during ABACUS surveys is provided in Fig. 6 and in the supplementary material (Figures S1 to S5) where MLD position is represented through the first derivative of potential density anomaly. This variable shows significant differences between glider and modelled values (except in 2016) in terms of both signal intensity and patterns along depth/latitude. On the other hand, a fine agreement exists between this glider derived information and the expected seasonal MLD location from climatology. D'Ortenzio et al. (2005), for example, report seasonal mean values of about 40 m in October and about 60 m in December in the AB (see their Fig. 1), which correspond well with glider observed results. This supports our hypothesis of a direct relationship between inaccurate MLD modelling and Chl-a discrepancies.

Nevertheless, the statistical results only provide a general picture of the complex scenario that characterizes the AB upper ocean dynamics. From this analysis it is extremely difficult to discuss how the model performances are related to other important factors that impact on the variability of the analysed physical and biological properties of the water column (e.g., seasonal variability, presence and evolution of small- and mesoscale structures), and provide a reliable explanation for

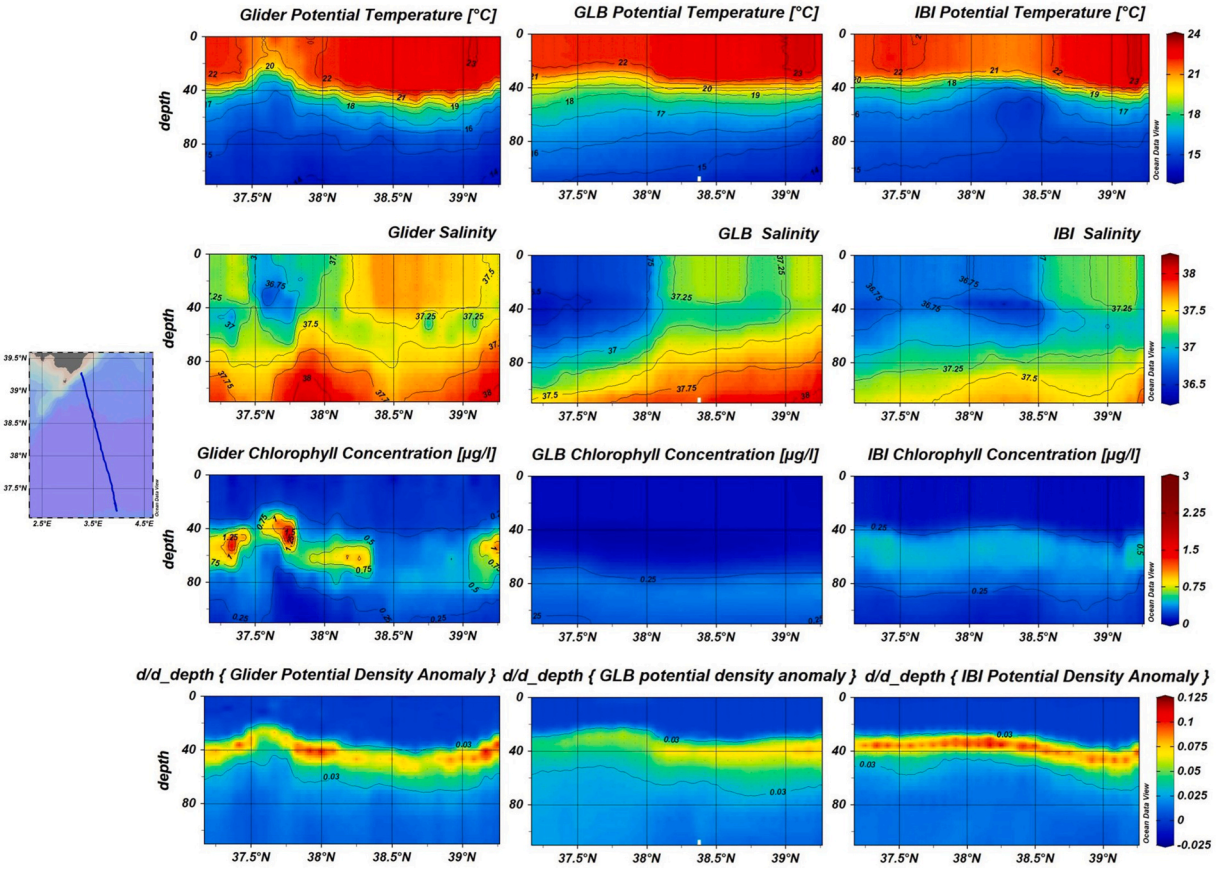

Fig. 6. Glider high resolution observations (left), GLB (middle) and IBI (right) simulations of (from top to bottom) potential temperature, salinity, chlorophyll concentration, and potential density anomaly derivative in the first 110 m of the water column during the ABACUS-2 survey (19–30 October 2015). The location of the analysed water column profiles is represented through blue dots in the left panel.

identifying ocean conditions during which each model is able (or not) to represent adequately the biomass stocks along the upper AB water column.

3.2. Latitudinal assessment: a case study

To enrich the discussion of the statistical analyses reported in the previous section, the upper ocean Chl-a patterns (0–110 m depth) observed during each glider survey has been also compared with GLB and IBI co-located sections across the Mallorca-AC chokepoint. Here we discuss the case study of the ABACUS 2 mission carried out during fall 2015 (Fig. 6). This survey provides the largest number of co-located points of comparison for our statistical analyses and is characterized by the higher values of Chl-a concentration registered during the ABACUS surveys. The other glider data sections along depth and latitude are indeed reported in the supplementary material in order to provide additional examples of the different performances of the GLB and IBI models in reproducing the spatial variability of the ABACUS observations.

Fig. 6 presents the potential temperature, salinity and Chl-a glider in situ observations (at about 5 km horizontal resolution) collected in the Algerian Basin during 19–30 October 2015. Potential density anomaly derivative along depth is also shown to provide information about the MLD. The measurement collected in the first 110 m depth along the monitoring line realized between the Island of Mallorca and the AC boundary are reported. An evident signature of Chl-a concentration maximum (ranging between 0.4 and 4.8 μg/l at different latitudes) is generally visible at about 40 - 70 m depth. Glider data also point out that the depth of maximum Chl-a is shallower where Chl-a concentration is higher. The maximum in Chl-a is likely associated with lower salinity values, an evident decrease in temperature and a local rise of isotherms. This happens in the southern part of the section (at 37.3 and 37.7 °N), in proximity of the oceanic front between the AC and the Mediterranean resident water masses (Arnone et al., 1990; Raimbault et al., 1993; Siokou-Frangou et al., 2010). Frontal zones are well known areas where secondary circulation (vertical velocities) can enhance the uplift of nutrients, increasing Chl-a production. A significant increase of Chl-a in the AC, for example, has been described by Moran et al. (2001) who investigated the biomass and production of phytoplankton and bacterioplankton in relation to the AC-related mesoscale structures during the ALGERS'96 cruise.

The presence of relatively low salinity filaments located at about 50–60 m depth can be also identified in the middle of the transect (at 38.2 °N) and in its northern part (at 38.7 and 39.1 °N). Once again, these sub-mesoscale filaments are associated with higher Chl-a concentration respect to the environ, even though the observed values are lower than along the southern border. This is a confirmation that oceanic fronts, as those associated to the AC, even at smaller spatial scales can constitute areas of very high Chl-a concentration.

CMEMS IBI and GLB model products co-located with these glider observations are also presented in Fig. 6. Numerical simulations are able to retrieve some characteristics observed along the water column, but important limitations appear due to the lower spatial resolution. Although the maximum of Chl-a concentration is usually reproduced well at about 50–70 m depth (see also supplementary material), both GLB and IBI outputs present large differences with glider measurements in terms of concentration that reach up to one order of magnitude (as for local maxima). Patterns of the Chl-a distribution are also very different, especially for GLB outputs.

Generally, IBI simulations provide better results in terms of both Chl-a concentration values and patterns. In particular, these outputs reproduce well the pattern of the local maxima of Chl-a concentration along the entire transect, especially in the northern and southern part of the section (i.e., at 39.2 and 37.7 °N).

Nevertheless, the retrieved simulations still include important issues that limit its capability to reproduce the ocean structure as needed for advanced ecological studies. Glider Chl-a concentration values are generally three-four times larger than IBI ones in the euphotic zone. These limits may be driven by the impossibility to identify and reproduce sub-mesoscale and small-scale structures that characterize the study area (e.g., the high salinity filaments observed in Fig. 6). Lower values are indeed provided by GLB products which fail in reproducing most of the spatial distribution of the Chl-a concentration, possibly due to the lower spatial resolution (1/4°).

Although it can be argued that models still capture the general picture of the ocean, the presence of sub-mesoscale structures is rather recurrent and cannot be disregarded in the AB. About one month later (1–8 December 2015), the northern part of the Mallorca-AC transect has been monitored again by the same ABACUS glider. In this second example, the signals of the small structures are still evident in terms of potential temperature, salinity and Chl-a concentration, even if they show different distribution and magnitude along the first 150 m (Fig. 7). Again, model products provide a quite different scenario of the water column patterns along depth, with IBI products showing the best performance compared with glider observations. GLB simulations indeed cannot provide reliable insights into the complex structure of the AB water column as seen by the glider.

4. Discussion and conclusions

Knowledge of the vertical structure of the bio-chemical properties of the ocean is crucial for the estimation of primary production, phytoplankton distribution, and biological modelling. Despite its growing importance, ocean biomass distribution inventory still needs improvements to represent a valid base for reliable and synoptic estimations. Chl-a concentration represents an excellent proxy for phytoplankton biomass and primary production, and offers the possibility to be monitored through several in situ and remote sensed approaches.

Satellite and classical in situ monitoring activities provide an important contribute to Chl-a estimations but do not resolve completely the spatial and temporal multi-resolution variability of ocean biomass distribution and dynamics along sea depth. Through the water column, in fact, the analysis of algal biomass is still hindered by practical difficulties. Satellite observations are strongly limited to penetration depth, while in situ samples are based on punctual measurements which are not easy to collect and result discontinue in space and time. Operational ocean modelling and data assimilation represent an alternative way to obtain a detailed description of the ocean structure with a continuous temporal coverage. Actually, models are able to describe the complex three-dimensional water column system, but often their outputs do not reproduce its sub-mesoscale and small-scale characteristics. This is crucial to understand ecological processes, so additional works are necessary for understanding to which extent different products can be used or not depending on the kind of study. The limits of model products are confirmed in this study where two daily CMEMS products (i.e., GLB and IBI) are compared with a set of high resolution measurements collected in the AB by gliders during the 2014–2018 time interval. The assessment of the CMEMS simulations show that daily in situ Chl-a concentration is not well represented by the analysed models, whose outputs show low or absent linear correlation with the co-located glider measurements and point out important differences in terms of both magnitude and vertical distribution. Amongst these products, the performed statistical analysis show that IBI model provide better results for the analysed case studies for all the available glider surveys.

The use of IBI model system as a useful tool to better understand the current state and changes in the marine biogeochemistry of Mediterranean waters has been already discussed in previous studies, e.g., by Gutknecht et al. (2019) which also indicated IBI weekly products as useful key variables for developing indicators to monitor the health of marine ecosystems. Nevertheless, section analyses along the glider transects confirm that IBI daily values are largely lower than those observed by gliders. Even though patterns of Chl-a maxima generally

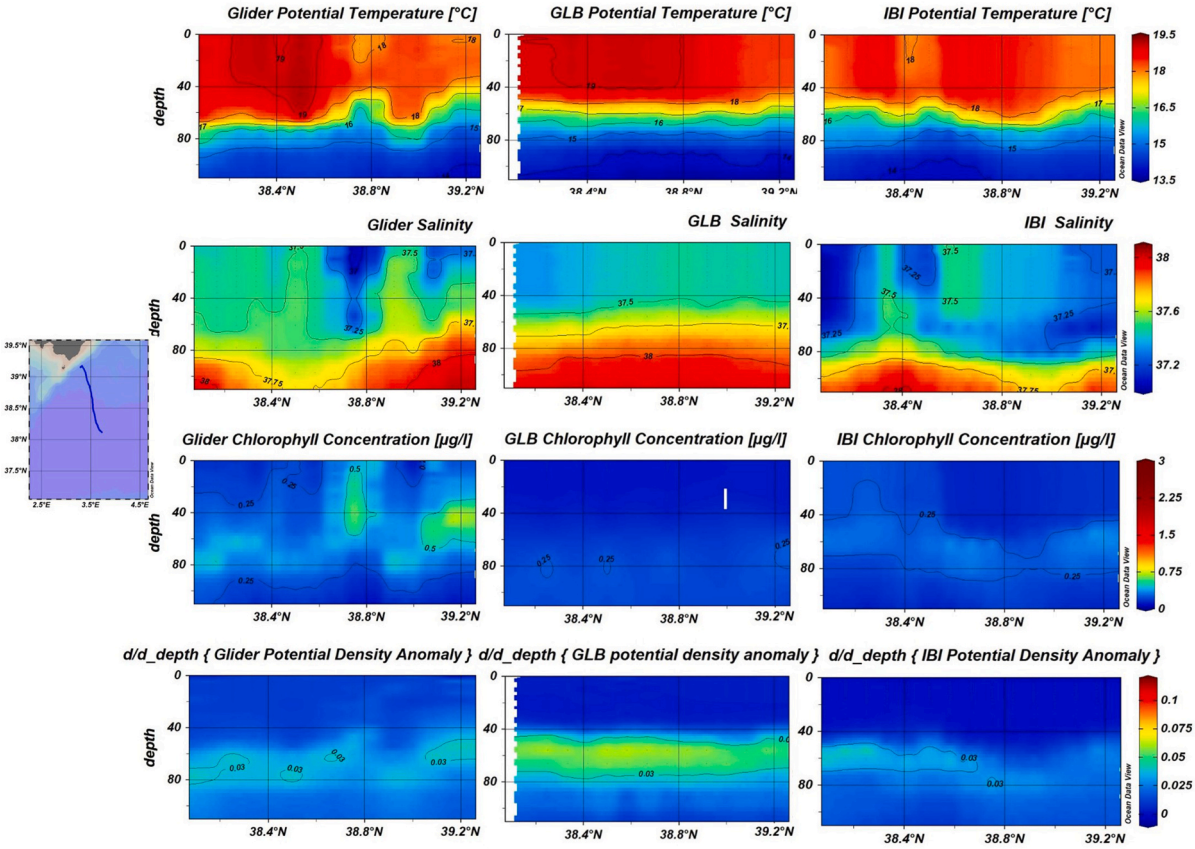

Fig. 7. As in Fig. 6 but for the ABACUS-2 survey second leg (1–8 December 2015).

correspond better than for GLB products, presumably, the effect of sub-mesoscale and small-scale variability that characterizes the study area is often missed.

In this context, an important role is played by the MLD variability that influences the biochemistry processes and could explain differences in Chl-a concentration described by models and in situ observations. Previous studies analysed the difference in terms of temperature and salinity patterns between CMEMS models and glider data along the ABACUS transects (Aulicino et al., 2018) and showed that MEDSEA analysis forecast outputs (produced by the Mediterranean Forecasting System, Lecci et al., 2019) represent the MLD variability of the study area better than IBI and GLB products, thus having a potential advantage in retrieving more reliable Chl-a concentration values. To date, as for MEDSEA, only monthly Chl-a products are available during the ABACUS campaigns, so that it is not possible to verify this hypothesis using co-located daily information.

Our findings suggest that if the MLD depth is well represented in the IBI and GLB outputs, then the modelled Chl-a is in better agreement with glider in situ observations. In this sense, a deeper quantitative analysis on the role of MLD is necessary to complement these results in a separate dedicated study.

In general, as previously assessed by several authors (e.g., Pascual et al., 2017; Hernandez-Lasheras and Mourre, 2018; Aguiar et al., 2020), the absence of a fine correspondence between modelled and measured Chl-a information stress the importance of further improving the initialization of CMEMS ocean models, usually based on other models having their own weaknesses, and of favouring the assimilation of high resolution in situ data in their systems in order to constrain the evolution of the Chl-a concentration along the water column in the AB.

The collection, and availability, of additional in situ observations is essential for feeding numerical models and retrieving more reliable outputs. Sampling resolution must be also appropriate in order to capture the sub-mesoscale and small-scale water column patterns which could be missed without the appropriate sampling acquisition strategy. This is vital for obtaining high resolution information adequate to improve model performance and advance on the characterisation and understanding of ocean processes and their role in the functioning of marine ecosystems. Maximizing spatial resolution cannot overlook a proper equilibrium with synopticity and time consumption that usually affect, for instance, lagrangian floats and ship-based measurements, respectively. For these reasons, it becomes necessary to find a complementary use of the available instruments and data, in order to supply the discontinuous nature of the actual in situ.

In this context, amongst other sources, cost efficient glider surveys can positively contribute to multiplatform data assimilation with important implications in terms of impact on regional modelling, improvement of climatology used in model initialization, and operational response to emergencies and sustainable management of the marine environment (Dobricic et al., 2010; Hayes et al., 2019; Tintoré et al., 2019). Additional insights about the usefulness of assimilating glider observations into regional models will be soon provided by forthcoming dedicated research activities by the present authors, which will focus on the assimilation of ABACUS physical and biogeochemical glider data into Mediterranean Sea regional models, e.g., The Western Mediterranean OPerational forecasting system (WMOP) implemented at SOCIB (Juza et al., 2016; Mourre et al., 2018).

Although gliders offer the opportunity to modulate the sampling strategy from survey to survey, and even during sea activities (i.e., through direct communication when surfacing), according to cost-efficiency constraints (e.g., days at sea, batteries, maritime traffic), unfortunately, at present time the limited number of available AUV platforms is largely insufficient to properly contribute to these goals. Furthermore, glider surveys are often dedicated to regional areas and target missions, so that acquired data are usually not assimilated (or

even not suitable to be assimilated) in ocean models. Thus, additional efforts are necessary to improve the fleet of operating gliders and increase the number of days at sea, as well as to foster and facilitate a closer cooperation between operational oceanographers, remote sensing experts and modellers.

In this direction, after the technical issues that halted the 2019 and 2020 campaigns, the ABACUS glider survey series will be back in 2021, enlarging its international and multidisciplinary network in order to complete more glider missions per year to monitor the AB seasonal and interannual variability. The increased number of repeated glider sections along the ABACUS monitoring line will improve the statistical relevancy of the differences and similarities with co-located model and satellite retrievals. Furthermore, the glider collection of physical and biological measurements will be enhanced by including new sensors which will provide additional information along the water column of the Mallorca–AC chokepoint, e.g., CDOM, PAR, microplastics, mammals (Suberg et al., 2014).

CRediT authorship contribution statement

Giuseppe Aulicino: Conceptualization, Data curation, Formal analysis, Investigation, Validation, Methodology, Supervision, Writing - original draft, Writing - review & editing. **Cinzia Cesarano:** Formal analysis, Investigation, Validation, Writing - review & editing. **Mohamed Zerrouki:** Data curation, Formal analysis, Investigation, Validation, Methodology, Writing - review & editing. **Simon Ruiz:** Investigation, Methodology, Writing - original draft, Writing - review & editing. **Giorgio Budillon:** Supervision, Funding acquisition, Writing - review & editing. **Yuri Cotroneo:** Conceptualization, Data curation, Formal analysis, Investigation, Methodology, Supervision, Funding acquisition, Writing - original draft, Writing - review & editing.

Declaration of Competing interest

The authors declare that they have no known competing financial interests or personal relationships that could have appeared to influence the work reported in this paper.

Acknowledgments

This work was realized in the framework of the PON R&I 2014–2020 “AIM – Attraction and International Mobility” at Università degli Studi di Napoli Parthenope. Glider missions were performed in the framework of the Algerian BAsin Circulation Unmanned Survey (ABACUS) observational projects. The ABACUS 1 missions (2014) were supported by the Joint European Research Infrastructure network for Coastal Observatories (JERICO) TransNational Access (TNA) third call (grant agreement no. 262584). The ABACUS 2 missions (2015) were realized through the SOCIB glider facility open access programme. The research leading to ABACUS 3 (2016) and ABACUS 4 (2017 and 2018) was supported by the European Union’s H2020 Framework Programme (h2020-INFRAIA-2014–2015) (JERICO—NEXT grant agreement no. 654410). The authors express their appreciation to the peer reviewers for their valuable comments and suggestions.

Supplementary materials

Supplementary material associated with this article can be found, in the online version, at doi:10.1016/j.ecolmodel.2021.109619.

References

Abdalla, S., et al., 2021. Altimetry for the future: building on 25 years of progress. Advan. Spac. Res. https://doi.org/10.1016/j.asr.2021.01.022.

Aguiar, E., Mourre, B., Juza, M., Reyes, E., Hernandez-Lasheras, J., Cutolo, E., Mason, E., Tintoré, J., 2020. Multi-platform model assessment in the western mediterranean sea: impact of downscaling on the surface circulation and mesoscale activity. Ocean Dyn. 70, 273–288. https://doi.org/10.1007/s10236-019-01317-8.

Arnone, R.A., Wiesenburg, D.A., Saunders, K.D., 1990. The origin and characteristics of the algerian current. J. Geophys. Res. 95, 1587–1598. https://doi.org/10.1029/JC095iC02p01587.

Aulicino, G., Cotroneo, Y., Lacava, T., Sileo, G., Fusco, G., Carlon, R., Satriano, V., Pergola, N., Tramutoli, V., Budillon, G., 2016. Results of the first wave glider experiment in the southern tyrrhenian sea. Adv. Oceanogr. Limnol. 7, 16–35. https://doi.org/10.4081/aiol.2016.5682.

Aulicino, G., Cotroneo, Y., Ruiz, S., Sanzhez-Román, A., Pascual, A., Fusco, G., Tintoré, J., Budillon, G., 2018. Monitoring the algerian basin through glider observations, satellite altimetry and numerical simulations along a saral/altika track. J. Mar. Syst. 179, 55–71. https://doi.org/10.1016/j.jmarsys.2017.11.006.

Aulicino, G., Cotroneo, Y., Olmedo, E., Cesarano, C., Fusco, G., Budillon, G., 2019. In situ and satellite sea surface salinity in the algerian basin observed through abacus glider measurements and bec smos regional products. Rem. Sens. 11, 1361. https://doi.org/10.3390/rs11111361.

Aumont, O., Ethé, C., Tagliabue, A., Bopp, L., Gehlen, M., 2015. PISCES-v2: an ocean biogeochemical model for carbon and ecosystem studies. Geosci. Mod. Dev. 8, 2465–2513. https://doi.org/10.5194/gmd-8-2465-2015.

Baladrón, A.A., Gutknecht, E., Aznar, R., Sotillo M.G., 2020. Product user manual for atlantic -iberian biscay irish- biogeochemistry multi-year non-assimilative hindcast product ibi_reanalysis_bio_005_003. http://marine.copernicus.eu/documents/PUM/CMEMS-IBI-PUM-005-003.pdf.

Barbier, E.B., 2019. The concept of natural capital. Oxf. Rev. Econ. Polic. 35 (1), 14–36. https://doi.org/10.1093/oxrep/gry028.

Barceló-Llull, B., Pascual, A., Díaz Barroso, L., Sánchez-Román, A., Casas, B., Muñoz, C., Torner, M., Alou, E., Cutolo, E., Mourre, B., Allen, J., Aulicino, G., Cabornero, A., Calafat, N., Capó, E., Cotroneo, Y., et al., 2020. PRE-SWOT cruise report. Mesoscale and sub-mesoscale vertical exchanges from multi-platform experiments and supporting modeling simulations. anticipating SWOT launch (CTM2016-78607-P),, 138. https://digital.csic.es/handle/10261/172644.

Bosse, A., Testor, P., Houpert, L., Damien, P., Prieur, L., Hayes, D., Taillandier, V., Durrieude Madron, X., D’Ortenzio, F., Coppola, L., Karstensen, J., Mortier, L., 2016. Scales and dynamics of submesoscale coherent vortices formed by deep convection in the northwestern mediterranean sea. J. Geophys. Res. 121, 7716–7742. https://doi.org/10.1002/2016JC012144.

Bosse, A., Testor, P., Mayot, N., Prieur, L., D’Ortenzio, F., Mortier, L., et al., 2017. A submesoscale coherent vortex in the ligurian sea: from dynamical barriers to biological implications. J. Geophys. Res. 122, 6196–6217. https://doi.org/10.1002/2016jc012634.

Bouzaiene, M., Menna, M., Poulain, P.M., Elhmaidi, D., 2018. Lagrangian dispersion characteristics in the western mediterranean. J. Mar. Res. 76, 139–161. https://doi.org/10.1357/002224018826473290.

Budillon, G., Cotroneo, Y., Aulicino, G., Fusco, G., Heslop, E., Torner, M., Tintoré, J., 2018. SOCIB tna abacus (version 1.0),socib, 10.25704/b200-3vf5.

Buongiorno Nardelli, B., Cavalieri, O., Rio, M.H., Santoleri, R., 2006. Subsurface geostrophic velocities inference from altimeter data: application to the sicily channel (mediterranean sea). J. Geophys. Res. 111, C04007. https://doi.org/10.1029/2005JC003191.

Buongiorno Nardelli, B., Guinehut, S., Verbrugge, N., Cotroneo, Y., Zambianchi, E., Iudicone, D., 2017. Southern ocean mixed-layer seasonal and interannual variations from combined satellite and in situ data. J. Geophys. Res. 122, 10042–10060.

Buongiorno Nardelli, B., 2020. A deep learning network to retrieve ocean hydrographic profiles from combined satellite and in situ measurements. Rem. Sens. 12 (19), 3151. https://doi.org/10.3390/rs12193151.

Buonocore, B., Cotroneo, Y., Capozzi, V., Aulicino, G., Zambardino, G., Budillon, G., 2020. Sea-Level variability in the gulf of naples and the “*acqua alta*” episodes in ischia from tide-gauge observations in the period 2002–2019. Wat. (Basel) 12, 2466. https://doi.org/10.3390/w12092466, 2020.

Castagno, P., de Ruggiero, P., Pierini, S., Zambianchi, E., De Alteris, A., De Stefano, M., Budillon, G., 2020. Hydrographic and dynamical characterisation of the bagnoli-coroglio bay (gulf of naples, tyrrhenian sea). Chem. Ecol. 36 (6), 598–618.

Celentano, P., Falco, P., Zambianchi, E., 2020. Surface connection between the ionian sea and different areas of the mediterranean derived from drifter data. Deep. Sea. Res. I. 166, 103431 https://doi.org/10.1016/j.dsr.2020.103431.

Coppola, L., Legendre, L., Lefevre, D., Prieur, L., Taillandier, V., Riquier, E.D., 2018. Seasonal and interannual variations of dissolved oxygen in the northwestern mediterranean sea (dyfamed site). Prog. Oceanogr. 162, 187–201. https://doi.org/10.1016/j.pocean.2018.03.001.

Cossarini, G., Solidoro, C., Fonda Umani, S., 2012. Dynamics of biogeochemical properties in temperate coastal areas of freshwater influence: lessons from the northern adriatic sea (gulf of trieste). Estuarine. Coast. Shel. Sci. 115, 63–74. https://doi.org/10.1016/j.ecss.2012.02.006.

Cotroneo, Y., Aulicino, G., Ruiz, S., Román, A.S., Tomàs, M.T., Pascual, A., Fusco, G., Heslop, E., Tintoré, J., Budillon, G., 2019. Glider data collected during the algerian basin circulation unmanned survey. Earth Syst. Sci. Data 11, 147–161. https://doi.org/10.5194/essd-11-147-2019.

Cotroneo, Y., Aulicino, G., Ruiz, S., Pascual, A., Budillon, G., Fusco, G., Tintoré, J., 2016. Glider and satellite high resolution monitoring of a mesoscale eddy in the algerian basin: effects on the mixed layer depth and biochemistry. J. Mar. Syst. 162, 73–88. https://doi.org/10.1016/j.jmarsys.2015.12.004.

D’Ortenzio, F., Iudicone, D., Montegut, C.D., Testor, P., Antoine, D., Marullo, S., Antoleri, R., Madec, G., 2005. Seasonal variability of the mixed layer depth in the mediterranean sea as derived from in situ profiles. Geophys. Res. Lett. 32 (12), L12605. https://doi.org/10.1029/2005 gl022463.

Daley, R., 1991. Atmospheric Data analysis. Cambridge. Cambridge University Press, p. 457.
Di Luccio, D., Riccio, A., Galletti, A., Laccetti, G., Lapegna, M., Marcellino, L., Kosta, S., Montella, R., 2020. Coastal marine data crowdsourcing using the internet of floating things: improving the results of a water quality model. Acce. IEEE. 8, 101209–101223, 2020.
Dobricic, S., Pinardi, N., Testor, P., Send, U., 2010. Impact of data assimilation of glider observations in the ionian sea (eastern mediterranean). Dyn. Atmos. Ocean. 50, 78–92. https://doi.org/10.1016/j.dynatmoce.2010.01.001.
Escudier, R., Mourre, B., Juza, M., Tintoré, J., 2016. Subsurface circulation and mesoscale variability in the algerian sub-basin from altimeter-derived eddy trajectories. J. Geophys. Res. 121, 6310–6322. https://doi.org/10.1002/2016JC011760.
Fernandez, E., Lellouche, J.M., 2018. Product user manual: for the global ocean sea physical reanalysis product global_reanalysis_phy_001_030.
Fusco, G., Manzella, G.M.R., Cruzado, A., Gacic, M., Gasparini, G.P., Kovacevic, V., Millot, C., Tziavos, C., Velasquez, Z.R., Walne, A., Zervakis, V., Zodiatis, G., 2003. Variability of mesoscale features in the mediterranean sea from xbt data analysis. Ann. Geophys. 21, 21–32. https://doi.org/10.5194/angeo-21-21-2003.
Fusco, G., Artale, V., Cotroneo, Y., Sannino, G., 2008. Thermohaline variability of mediterranean water in the gulf of cádiz, 1948–1999. Deep-Sea Res. I. 55, 1624–1638.
Garau, B., Ruiz, S., Zang, G.W., Heslop, E., Kerfoot, J., Pascual, A., Tintoré, J., 2011. Thermal lag correction on Slocum ctd glider data. J. Atmos. Ocean. Tech. 28, 1065–1074.
Garreau, P., Dumas, F., Louazel, S., Correard, S., Fercocq, S., Le Menn, M., Serpette, A., Garnier, V., Stegner, A., Le Vu, B., et al., 2020. PROTEVS−MED field experiments: very high−resolution hydrographic surveys in the western mediterranean sea. Earth Syst. Sci. Data. 12 (1), 441–456. https://doi.org/10.5194/essd-12-441-2020.
Groom, S., Sathyendranath, S., Ban, Y., Bernard, S., Brewin, R., Brotas, V., Brockmann, C., Chauhan, P., Choi, J., Chuprin, A., et al., 2019. Satellite ocean colour: current status and future perspective. Front. Mar. Sci. 6, 485. https://doi.org/10.3389/fmars.2019.00485.
Gueye, M.B., Niang, A., Arnault, S., Thiria, S., Crépon, M., 2014. Neural approach to inverting complex system: application to ocean salinity profile estimation from surface parameters. Comput. Geosci. 72, 201–209. https://doi.org/10.1016/j.cageo.2014.07.012.
Gutknecht, E., Reffray, G., Mignot, A., Dabrowski, T., Sotillo, M.G., 2019. Modelling the marine ecosystem of iberia–biscay–ireland (ibi) european waters for cmems operational applications. Ocean Sci. 15, 1489–1516. https://doi.org/10.5194/os-15-1489-2019.
Hayes, D.R., Dobricic, S., Gildor, H., Matsikaris, A., 2019. Operational assimilation of glider temperature and salinity for an improved description of the cyprus Eddy. Deep-Sea Res. Part II 164, 41–53. https://doi.org/10.1016/j.dsr2.2019.05.015.
Hernandez-Lasheras, J., Mourre, B., 2018. Dense Ctd survey versus glider fleet sampling: comparing data assimilation performance in a regional ocean model west of sardinia. Ocean Sci. 14, 1069–1084. https://doi.org/10.5194/os-14-1069-2018.
Heslop, E.E., Ruiz, S., Allen, J., López-Jurado, J.L., Renault, L., Tintoré, J., 2012. Autonomous underwater gliders monitoring variability at chokepoints in our ocean system: a case study in the western mediterranean sea. Geophys. Res. Lett. 39, L20604, 20.
Krauzig, N., Falco, P., Zambianchi, E., 2020. Contrasting surface warming of a marginal basin due to large-scale climatic patterns and local forcing. Sci. Rep. 10, 17648. https://doi.org/10.1038/s41598-020-74758-7.
Juza, M., Escudier, R., Pascual, A., Pujol, M.I., Taburet, G., Troupin, C., Mourre, B., Tintoré, J., 2016. Impacts of reprocessed altimetry on the surface circulation and variability of the western alboran gyre. Adv. Space Res. 58 (3), 277–288. https://doi.org/10.1016/j.asr.2016.05.026.
Leach, K., Grigg, A., O'Connor, B., Brown, C., Vause, J., Gheyssens, J., Weatherdon, L., Halle, M., Burgess, N.D., Fletcher, R., et al., 2019. A common framework of natural capital assets for use in public and private sector decision making. Ecosyst. Serv. 36, 100899 https://doi.org/10.1016/j.ecoser.2019.100899.
Lecci R., Salon G., Bolzon G., Cossarini G., 2019. Product user manual for mediterranean sea biochemical analysis and forecasting product, cmems-med-pum-006-014.
Lévy, M., Franks, P.J.S., Smith, K.S., 2018. The role of submesoscale currents in structuring marine ecosystems. Nat. Commun. 9, 4758. https://doi.org/10.1038/s41467-018-07059-3.
Mahadevan, A., D'Asaro, E., Perry, M.J., Lee, C., 2012. Eddy-driven stratification initiates north atlantic spring phytoplankton blooms. Sci. 337 (6090), 54–58. https://doi.org/10.1126/science.1218740.
Mangoni, O., Saggiomo, V., Bolinesi, F., Margiotta, F., Budillon, G., Cotroneo, Y., Misic, C., Rivaro, P., Saggiomo, M., 2017. Phytoplankton blooms during austral summer in the ross sea, antarctica: driving factors and trophic implications. PLoS ONE 12 (4), e0176033. https://doi.org/10.1371/journal.pone.0176033.
MERP, 2019. Marine ecosystems research programme - final report. https://www.marine-ecosystems.org.uk/Resources/Reports.
Millot, C., 1999. Circulation in the western mediterranean sea. J. Mar. Syst. 20, 423–442.
Misic, C., Covazzi Harriague, A., Mangoni, O., Aulicino, G., Castagno, P., Cotroneo, Y., 2017. Effects of physical constraints on the lability of pom during summer in the ross sea. J. Mar. Syst. 166, 132–143. https://doi.org/10.1016/j.jmarsys.2016.06.012.
Morel, A., Berthon, J.F., 1989. Surface pigments, algal biomass profile, and potential production of the eutrophis layer: relationships reinvestigated in view of remote applications. Limnol. Oceanogr. 34, 1545–1562.
Mourre, B., Aguiar, E., Juza, M., Hernandez-Lasheras, J., Reyes, E., Heslop, E., Escudier, R., Cutolo, E., Ruiz, S., Pascual, A., Tintoré, J., 2018. Assesment of high-resolution regional ocean prediction systems using multiplatform observations: illustrations in the western mediterranean sea. In: New Frontiers in Operational Oceanography, 663–694. GODAE Ocean View. 10.17125/gov2018.
Niewiadomska, K., Claustre, H., Prieur, L., D'Ortenzio, F., 2008. Submesoscale physical-biogeochemical coupling across the ligurian current (northwestern mediterranean) using a bio-optical glider. Limnol. Oceanogr. 53 (5), 2210–2225. https://doi.org/10.4319/lo.2008.53.5_part_2.2210 part 2.
Olita, A., Ribotti, A., Sorgente, R., Fazioli, L., Perilli, A., 2011. SLA-chlorophyll-a variability and covariability in the algero-provençal basin (1997–2007) through combined use of eof and wavelet analysis of satellite data. Ocean Dyn. 61, 89–102. https://doi.org/10.1007/s10236-010-0344-9, 2011.
Olita, A., Sparnocchia, S., Cusí, S., Fazioli, L., Sorgente, R., Tintoré, J., 2014. Ocean Sci 10, 657–666. https://doi.org/10.5194/os-10-657-2014.
Pardo-Iguzquiza, E., 1998. Comparison of geostatistical methods for the estimation of the areal average climtatological rainfall mean using data on precipitation and topography. Int. J. Climatol. 18, 1031–1047.
Pascual, A., Bouffard, J., Ruiz, S., Buongiorno Nardelli, B., Vidal-Vijande, E., Escudier, R., Sayol, J.M., Orfila, A., 2013. Recent improvements in mesoscale characterization of the western mediterranean sea: synergy between satellite altimetry and other observational approaches. Sci. Mar. 77, 19–36. https://doi.org/10.3989/scimar.03740.15A.
Pascual, A., Ruiz, S., Olita, A., Troupin, C., Claret, M., Casas, B., Mourre, B., Poulain, P. M., Tovar-Sanchez, A., Capet, A., Mason, E., Allen, J.T., Mahadevan, A., Tintoré, J., 2017. A multiplatform experiment to unravel Meso- and submesoscale processes in an intense front (alborex). front. Mar. Sci. 4, 39. https://doi.org/10.3389/fmars.2017.00039.
Payne, T.E., Gregory, S.A., Dentamaro, A., Ernst, M., Hollon, J., Kruchten, A., Chaudhary, A.B., Dao, P.D., 2019. Development and evaluation of new methods for estimating albedo-areas for three-axis stabilized geosynchronous satellites. J. Astronaut. Sci. 66, 170–191. https://doi.org/10.1007/s40295-018-00143-2.
Perruche C., 2019. Product user manual for the global ocean biogeochemistry hindcast global_reanalysis_bio_001_0292019. http://marine.copernicus.eu/documents/PUM/CMEMS-GLO-PUM-001-029.pdf.
Pessini, F., Olita, A., Cotroneo, Y., Perilli, A., 2018. Mesoscale eddies in the algerian basin: do they differ as a function of their formation site? Ocean Sci. 14, 669–688. https://doi.org/10.5194/os-14-669-2018, 2018.
Pessini, F., Cotroneo, Y., Olita, A., Sorgente, R., Ribotti, A., Jendersie, S., Perilli, A., 2020. Life history of an anticyclonic eddy in the algerian basin from altimetry data, tracking algorithm and in situ observations. J. Mar. Syst. 207, 103346 https://doi.org/10.1016/j.jmarsys.2020.103346.
Picone, F., Buonocore, E., D'Agostaro, R., Donati, S., Chemello, R., Franzese, P.P., 2017. Integrating natural capital assessment and marine spatial planning: a case study in the mediterranean sea. Ecol. Model. 361, 1–13. https://doi.org/10.1016/j.ecolmodel.2017.07.029.
Poulain, P.M., Menna, M., Mauri, E., 2012. Surface geostrophic circulation of the mediterranean sea derived from drifter and satellite altimeter data. J. Phys. Oceanogr. 42, 973–990. https://doi.org/10.1175/JPO-d-11-0159.1.
Raimbault, P., Coste, B., Boulhadid, M., Boudjellal, B., 1993. Origin of high phytoplankton concentration in deep chlorophyll maximum (dcm) in a frontal region of the southwestern mediterranean sea (algerian current). Deep-Sea Res. I, Oceanogr. Res. Pap. 40, 791–804.
Richardson, A.J., Pfaff, M.C., Field, J.G., Silulwane, N.F., Shillington, F.A., 2002. Identifying characteristic clorophyll-a profiles in the coastal domain using an artificial neural network. J. Plankt. Res. 24, 1289–1303.
Rivaro, P., Ianni, C., Langone, L., Ori, C., Aulicino, G., Cotroneo, Y., Saggiomo, M., Mangoni, O., 2017. Physical and biological forcing of mesoscale variability in the carbonate system of the ross sea (antarctica) during summer 2014. J. Mar. Syst. 166, 144–158. https://doi.org/10.1016/j.jmarsys.2015.11.002.
Rivaro, P., Ardini, F., Grotti, M., Aulicino, G., Cotroneo, Y., Fusco, G., Mangoni, O., Bolinesi, F., Saggiomo, M., Celussi, M., 2019a. Mesoscale variability related to iron speciation in a coastal ross sea area (antarctica) during summer 2014. Chem. Ecol. 35, 1–19. https://doi.org/10.1080/02757540.2018.1531987.
Rivaro, P., Ianni, C., Raimondi, L., Manno, C., Sandrini, S., Castagno, P., Cotroneo, Y., Falco, P., 2019b. Analysis of physical and biogeochemical control mechanisms on summertime surface carbonate system variability in the western ross sea (antarctica) using in situ and satellite data. Rem. Sens. 11, 238. https://doi.org/10.3390/rs11030238.
Robinson, A.R., 1983. Eddies in Marine Science. Springer Verlag, New York, 609.
Robinson, M., Golnaraghi, A., 1994. Ocean Processes in Climate dynamics: Global and Mediterranean examples, the Physical and Dynamical Oceanography of the Mediterranean Sea. Kluwer Academic Publishing, Dordrecht.
Ruiz, S., Font, J., Emelianov, M., Isern-Fontanet, I., Millot, C., Salas, J., Taupier-Letage, I., 2002. Deep structure of an open sea eddy in the algerian basin. J. Mar. Syst. 33-34, 179–195. https://doi.org/10.1016/S0924-7963(02)00058-1.
Ruiz, S., Pascual, A., Garau, B., Pujol, M.I., Tintoré, J., 2009. Vertical motion in the upper ocean from glider and altimetry data. Geophys. Res. Lett. 36 (14), L14607. https://doi.org/10.1029/2009GL038569.
Ruiz, S., Claret, M., Pascual, A., Olita, A., Troupin, C., Capet, A., Tovar-Sanchez, A., Allen, J., Poulain, P., Tintore, J., Mahadevan, A., 2019. Effects of oceanic mesoscale and submesoscale frontal processes on the vertical transport of phytoplankton. J. Geophys. Res. Oceans 124 (8), 5999–6014. https://doi.org/10.1029/2019JC015034.
Sammartino, M., Marullo, S., Santoleri, R., Scardi, M., 2018. Modelling the vertical distribution of phytoplankton biomass in the mediterranean sea from satellite data: a neural network approach. Remote Sens 10, 1666. https://doi.org/10.3390/rs10101666.

Sánchez-Román, A., Gómez-Navarro, L., Fablet, R., et al., 2019. Rafting behaviour of seabirds as a proxy to describe surface ocean currents in the balearic sea. Sci. Rep. 9, 17775. https://doi.org/10.1038/s41598-018-36819-w.

Sathyendranath, S., Aiken, J., Alvain, S., Barlow, R., Bouman, H., Bracher, A., Brewin, R., Bricaud, A., Brown, C.W., Ciotti, A.M., et al., 2014. Phytoplankton functional types from space. Rep. Inter. Ocean-Colour Coordinat. Grp. (IOCCG) 15, 1–156. Dartmouth, NS, Canada.

Sathyendranath, S., Brewin, R.J.W., Jackson, T., Mélin, F., Platt, T., 2017. Ocean-colour products for climate-change studies: what are their ideal characteristics? Rem. Sens. Environ. 203, 125–138. https://doi.org/10.1016/j.rse.2017.04.017.

Sauzède, R., Claustre, H., Uitz, J., Jamet, C., Dall'Olmo, G., D'Ortenzio, F., Gentili, B., Poteau, A., Schmechtig, C., 2016. A neural network-based method for merging ocean color and Argo data to extend surface biooptical properties to depth: retrieval of the particulate backscattering coefficient. J. Geophys. Res. Oceans 121. https://doi.org/10.1002/2015JC011408.

Scardi, M., 2001. Advances in neural network modeling of phytoplankton primary production. Ecol. Model. 146, 33–45.

Siokou-Frangou, I., Christaki, U., Mazzocchi, M.G., Montresor, M., Ribera d'Alcalá, M., Vaqué, D., Zingone, A., 2010. Plankton in the open mediterranean sea: a review. Biogeosci. 7, 1543–1586. https://doi.org/10.5194/bg-7-1543-2010.

Strömberg, K.H.P., Smyth, T.J., Allen, J.I., Pitois, S., O'Brien, T.D., 2009. Estimation of global zooplankton biomass from satellite ocean color. J. Mar. Syst. 78, 18–27. https://doi.org/10.1016/j.jmarsys.2009.02.004.

Suberg, L., Wynn, R.B., Kooij, J., Fernand, L., Fielding, S., Guihen, D., et al., 2014. Assessing the potential of autonomous submarine gliders for ecosystem monitoring across multiple trophic levels (plankton to cetaceans) and pollutants in shallow shelf seas. Meth. Oceanogr. 10, 70–89. https://doi.org/10.1016/j.mio.2014.06.002.

Taillandier, V., Prieur, L., D'Ortenzio, F., Ribera d'Alcala, M., Pulido-1185 Villena, E., 2020. Profiling float observation of thermohaline staircases in the western Mediterranean Sea and impact on nutrient fluxes. Biogeosci. 17, 3343–3366.

Taupier-Letage, I., 1988. Biodynamique du bassin algerien: estimation de la reponse biologique à certaines structures moyenne echelle par teledetection (avhrr et czcs) et mesures in situ. In: Ph.D. thesis. Univ. d'Aix-Marseille II, Marseille (France), 120 pp.

Taupier-Letage, I., Puillat, I., Raimbault, P., Millot, C., 2003. Biological response to mesoscale eddies in the algerian basin. J. Geophys. Res. 108, 3245–3267.

Testor, P., Send, U., Gascard, J.C., Millot, C., Taupier-Letage, I., Beranger, K., 2005. The mean circulation of the Southwestern Mediterranean Sea: algerian gyres. J. Geophys. Res. 110, C11017. https://doi.org/10.1029/2004JC002861.

Tintoré, J., Pinardi, N., Álvarez-Fanjul, E., Aguiar, E., Álvarez-Berastegui, D., Bajo, M., et al., 2019. Challenges for sustained observing and forecasting systemsin the mediterranean sea. front. Mar. Sci. 6, 568. https://doi.org/10.3389/fmars.2019.00568.

Vidal-Vijande, E., Pascual, A., Barnier, B., Molines, J.M., Tintoré, J., 2011. Analysis of a 44-year hindcast for the mediterranean sea: comparison with altimetry and in situ observations. Sci. Mar. 75, 71–86. https://doi.org/10.3989/scimar.2011.75n1071, 2011.

Webb, D.C., Simonetti, P.J., Jones, C.P., 2001. SLOCUM: an underwater glider propelled by environmental energy. IEEE. J. Oceani. Eng. 26, 447–452. https://doi.org/10.1109/48.972077.

Zambianchi, E., Trani, M., Falco, P., 2017. Lagrangian transport of marine litter in the mediterranean sea. Front. Environ. Sci. https://doi.org/10.3389/fenvs.2017.00005.